

# Lawrence Berkeley National Laboratory

## LBL Publications

### Title

Methane Carboxylation Using Electrochemically Activated Carbon Dioxide.

### Permalink

<https://escholarship.org/uc/item/2sx7r0f1>

### Journal

Angewandte Chemie, 62(27)

### Authors

Yuan, Yucheng

Zhang, Yuhan

Li, Haoyi

et al.

### Publication Date

2023-07-03

### DOI

10.1002/anie.202305568

Peer reviewed



# HHS Public Access

Author manuscript

*Angew Chem Int Ed Engl.* Author manuscript; available in PMC 2024 July 03.

Published in final edited form as:

*Angew Chem Int Ed Engl.* 2023 July 03; 62(27): e202305568. doi:10.1002/anie.202305568.

## Methane Carboxylation Using Electrochemically Activated Carbon Dioxide

Yucheng Yuan,

Yuhan Zhang,

Haoyi Li,

Muchun Fei,

Hongna Zhang,

John Santoro,

Dunwei Wang

Department of Chemistry, Boston College, 2609 Beacon St., Chestnut Hill MA 02467, United States

### Abstract

Direct synthesis of  $\text{CH}_3\text{COOH}$  from  $\text{CH}_4$  and  $\text{CO}_2$  is an appealing approach for the utilization of two potent greenhouse gases that are notoriously difficult to activate. In this *Communication*, we report an integrated route to enable this reaction. Recognizing the thermodynamic stability of  $\text{CO}_2$ , our strategy sought to first activate  $\text{CO}_2$  to produce  $\text{CO}$  (through electrochemical  $\text{CO}_2$  reduction) and  $\text{O}_2$  (through water oxidation), followed by oxidative  $\text{CH}_4$  carbonylation catalyzed by Rh single atom catalysts supported on zeolite. The net result was  $\text{CH}_4$  carboxylation with 100% atom economy.  $\text{CH}_3\text{COOH}$  was obtained at a high selectivity (>80%) and good yield (*ca.* 3.2 mmol/ $\text{g}_{\text{cat}}$  in 3 h). Isotope labelling experiments confirmed that  $\text{CH}_3\text{COOH}$  is produced through the coupling of  $\text{CH}_4$  and  $\text{CO}_2$ . This work represents the first successful integration of  $\text{CO}/\text{O}_2$  production with oxidative carbonylation reaction. The result is expected to inspire more carboxylation reactions utilizing preactivated  $\text{CO}_2$  that take advantage of both products from the reduction and oxidation processes, thus achieving high atom efficiency in the synthesis.

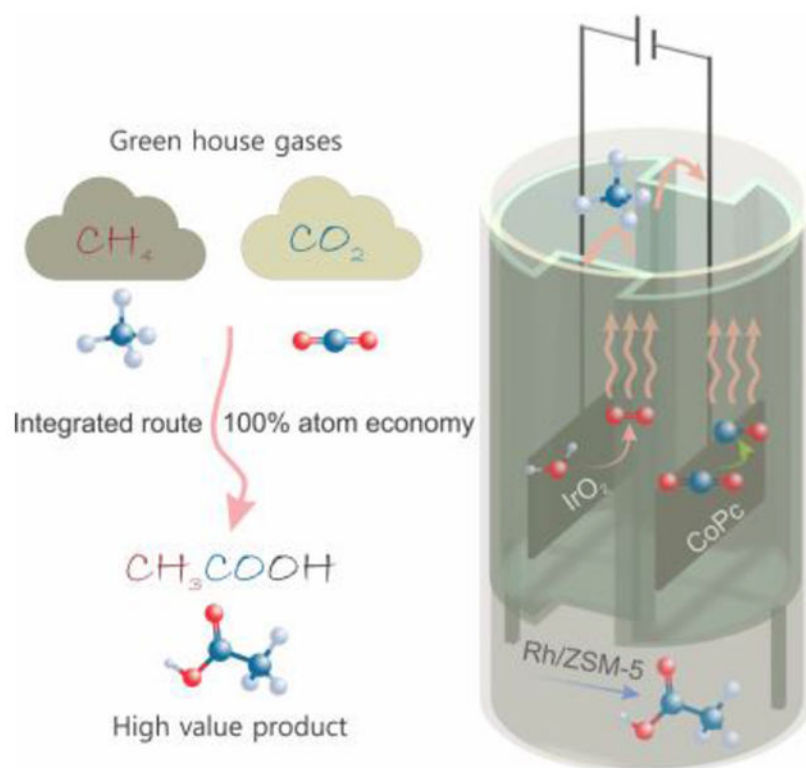
### Graphical Abstract

---

dunwei.wang@bc.edu .

Supporting information for this article is given via a link at the end of the document.

Twitter: @Wanggroup\_BC



Direct synthesis of  $\text{CH}_3\text{COOH}$  from  $\text{CH}_4$  and  $\text{CO}_2$  is made possible. The process first activates  $\text{CO}_2$  by electrochemistry, producing  $\text{CO}$  and  $\text{O}_2$ . It is followed by oxidative  $\text{CH}_4$  carbonylation catalyzed by  $\text{Rh}$  single atom catalysts. The net result is  $\text{CH}_4$  carboxylation with 100% atom economy.

## Keywords

electrochemistry; catalysis; acetic acid synthesis; methane carbonylation;  $\text{CO}_2$  utilization

As an abundant natural resource, methane ( $\text{CH}_4$ ) is an appealing feedstock for producing high-value hydrocarbons such as liquid fuels and other chemicals. However, due to the notorious difficulties in selectively activating the C-H bonds in  $\text{CH}_4$ , its large-scale industrial utilization has been limited to first reforming it to produce syngas ( $\text{CO}$  and  $\text{H}_2$ ), followed by subsequent processes often broadly referred to as the Fischer-Tropsch transformation to form liquid hydrocarbons.<sup>[1]</sup> Consider the production of  $\text{CH}_3\text{COOH}$  as one example, which is widely used in food industry and medicinal applications as well as a precursor for the synthesis of various chemicals, including vinyl acetate monomer, esters, acetic anhydride, and numerous polymeric materials.<sup>[2]</sup> Two industrial methods prevail in the efforts of synthesizing this important intermediate in bulk quantities, namely the Monsanto process and the Cativa process (Figure 1).<sup>[3]</sup> While different in the catalysts they employ, both processes share many similarities. For instance, the key to both processes is the carbonylation step, which uses  $\text{CO}$  as a precursor. Moreover, they both use  $\text{CH}_3\text{OH}$  as the other precursor, the synthesis of which ( $\text{CO}$  hydrogenation) is in turn enabled by steam

methane reforming (SMR). Recognizing the undesired issues of SMR such as high energy intensity and low efficiency, researchers have sought to achieve direct methane carbonylation with the help of molecular oxygen.<sup>[4]</sup> While exciting progress has been made toward this direction, the process still relies on pre-synthesized toxic CO as a carbonylation precursor, whose industrial synthesis requires SMR.

A careful examination of the molecular structure of CH<sub>3</sub>COOH reveals that it would be possible to prepare it by directly coupling CH<sub>4</sub> and CO<sub>2</sub> with 100% atom efficiency (Figure 1). Given the abundance of both molecules in nature and their potent greenhouse effects, such a route would be of great interest. Indeed, several studies have already been carried out to investigate this possibility computationally using density functional theory (DFT).<sup>[5]</sup> It has been found that the direct route of CH<sub>3</sub>COOH synthesis through CH<sub>4</sub> and CO<sub>2</sub> coupling is thermodynamically unfavorable under practical conditions.<sup>[6]</sup> Experimental demonstrations of direct CH<sub>4</sub> carboxylation using CO<sub>2</sub> as a source have been scarce, and the few existing catalytic systems suffer poor controls over the product selectivity.<sup>[7]</sup> At the heart of the challenge is the need to simultaneously activate two highly stable molecules in a controllable fashion. On the other hand, recent literatures have seen significant efforts and successes to activate CH<sub>4</sub> or CO<sub>2</sub>, albeit under very different conditions.<sup>[4a, 4b, 8]</sup> It is, therefore, conceivable to take advantage of these recent developments in the two separate subfields and enable direct synthesis of CH<sub>3</sub>COOH using CH<sub>4</sub> and CO<sub>2</sub> as the only precursors. It is within this context that we have developed the present work. As shown in Figure 1, we capitalized on recent successes in two different directions, namely selective CO<sub>2</sub> reduction and oxidative CH<sub>4</sub> carbonylation, and achieved atomically efficient synthesis of CH<sub>3</sub>COOH with high selectivity.

Among the two precursors, CH<sub>4</sub> and CO<sub>2</sub>, the latter is difficult to activate because of its thermodynamic stability, whereas the activation of the former is primarily due to the high kinetic barriers. We were, therefore, inspired to first seek to address the thermodynamic challenge. Fortunately, this topic (the activation of CO<sub>2</sub>) has been intensely studied and extensively reported in the literature.<sup>[8c, 9]</sup> For instance, electrochemical CO<sub>2</sub> reduction reaction (CO<sub>2</sub>RR) is one of the most published research topics lately. Among the various products, CO can be obtained from CO<sub>2</sub>RR with a high selectivity (>90%) and yield.<sup>[10]</sup> Nevertheless, this important feedstock has been rarely utilized after its generation from CO<sub>2</sub>RR.<sup>[9c, 11]</sup> Skrydstrup *et al.* demonstrated the coupling of CO production from CO<sub>2</sub>RR and Pd-catalysed carbonylation reactions in a seminal work.<sup>[11]</sup> However, organic solvents (*e.g.*, N,N-dimethylformamide) and sacrificial reagents (*e.g.*, triethylamine) were employed to facilitate the counter reaction for CO<sub>2</sub>RR. As a result, the products on the anodes were not utilized and valuable reagents were sacrificed, making it an unsustainable way of valorizing CO<sub>2</sub>. Broadly speaking, oxidative carbonylation has been recognized as a promising strategy for CO<sub>2</sub> utilization without sacrificing the counter reaction but has not been achieved yet.<sup>[9c]</sup> Thus, we demonstrated the first example of integrating CO/O<sub>2</sub> production with oxidative carbonylation herein. When coupled with H<sub>2</sub>O oxidation at the counter electrode, the reaction can produce CO and O<sub>2</sub> in stoichiometry. The mixture (CO:O<sub>2</sub> = 2:1) can then be utilized to activate CH<sub>4</sub> for the production of CH<sub>3</sub>COOH with 100% atom efficiency. We specifically employed this setup and carefully chose catalysts for the three reactions involved with the goal to demonstrate the feasibility of carboxylation

reaction of CH<sub>4</sub> by CO<sub>2</sub> in an integrated fashion. For this body of work, commercially available cobalt(II) phthalocyanine (CoPc) complexes<sup>[10b, 12]</sup> and IrO<sub>2</sub><sup>[13]</sup> were chosen as the catalysts for CO<sub>2</sub>RR and oxygen evolution reaction (OER), respectively, as shown in Figure 1, **right** (also see the reactor setup in Figure S1 in Supporting Information, SI). The former was chosen for its easy access and high selectivity toward CO as well as its tolerance of O<sub>2</sub> with pressurized CO<sub>2</sub> and high stability, and the latter was selected for its high activity and stability toward H<sub>2</sub>O oxidation. With a constant current density of 11.1 mA/cm<sup>2</sup>, the potential difference between the cathode and anode remained relatively stable at *ca.* 2.9 V for at least 26 h, indicating the electrochemical system was stable under our experimental conditions (Figure 2, top, see linear sweep voltammetry (LSV) curves of CoPc in Figure S2). The CO and O<sub>2</sub> products were monitored by a gas chromatography equipped with a flame ionization detector (GC-FID) for CO and thermal conductivity detector (GC-TCD) for O<sub>2</sub> quantifications, respectively. The partial pressures of these products were then calculated, and the data are shown in Figure 2 (bottom). It was observed that their ratio (CO:O<sub>2</sub>) was stable throughout the reaction. The partial pressures of CO and O<sub>2</sub> ( $P_{\text{CO}}$  and  $P_{\text{O}_2}$ ) reached *ca.* 4 bar and 2 bar, respectively, at 22 h. Presumably due to the competitive O<sub>2</sub> reduction reaction, the faradaic efficiency for CO<sub>2</sub>RR was relatively low (*ca.* 30%), which was comparable with that under a similar volume fraction of O<sub>2</sub> in previous reports.<sup>[14]</sup> As will be further discussed later in this *Communication*, the yield of H<sub>2</sub> was *ca.* 0.6 bar under this condition. Because previous literature has shown that such pressures are suitable for CH<sub>4</sub> carbonylation reactions,<sup>[4a]</sup> we employed 22 h as the reaction time for CO<sub>2</sub>RR for the remainder of this study.

To perform oxidative CH<sub>4</sub> carbonylation in the second step, we prepared atomically dispersed rhodium (Rh) catalyst on a zeolite support (0.5 wt% Rh-ZSM-5) following a previous report by Flytzani-Stephanopoulos and treated the as-synthesized catalyst with H<sub>2</sub> at 550 °C for 3 h (Figure S3).<sup>[4a]</sup> Diffuse reflectance infrared Fourier transform spectroscopy study of CO (CO-DRIFTS) on the H<sub>2</sub> treated catalyst featured two characteristic peaks at 2114 cm<sup>-1</sup> and 2048 cm<sup>-1</sup>, which are attributed to symmetrical and asymmetrical stretching of CO adsorbed onto isolated mononuclear Rh<sup>I</sup>(CO)<sub>2</sub> species (Figure S4).<sup>[4a]</sup> Another important note we have taken from the previous report was the reaction conditions, where the optimum ratio between the reactants was CH<sub>4</sub>:CO:O<sub>2</sub> = 20:5:2. Away from these ratios, further increasing O<sub>2</sub> would lead to overoxidation and poorer selectivity towards CH<sub>3</sub>COOH, and reducing it would result in a lower yield. A constraint we faced in our experiments is the ratio between CO and O<sub>2</sub> (2:1), which is fixed as determined by the stoichiometry of CO<sub>2</sub> reduction coupled with H<sub>2</sub>O oxidation. We thus sought to observe how varying the partial pressure of CH<sub>4</sub> with a fixed CO:O<sub>2</sub> ratio might influence the reactions. As shown in Figure 3a and Figure S5a, when  $P_{\text{CO}}$  and  $P_{\text{O}_2}$  were fixed at 4 bar and 2 bar, respectively, there was a clear trend of increased CH<sub>3</sub>COOH production with the increase of  $P_{\text{CH}_4}$  up to 18 bar, beyond which higher  $P_{\text{CH}_4}$  led to reduced CH<sub>3</sub>COOH yield. We note that there should be additional room for further optimization with regard to the yield as normalized to the catalyst loading. For instance, Flytzani-Stephanopoulos *et al.* have shown that the catalyst performance could be readily improved by repeating the impregnation process multiple times.<sup>[4a]</sup> Another figure of merit we closely monitored was the selectivity toward CH<sub>3</sub>COOH among all liquid products. It is observed in Figure 3a that at 85%, it

is comparable to the benchmark reported previously.<sup>[4a, 4b]</sup> This selectivity was obtained at  $P_{\text{CH}_4} = 18$  bar; further increasing  $\text{CH}_4$  resulted in reduced selectivity toward  $\text{CH}_3\text{COOH}$ . The last set of parameters we have varied was the total pressure. It is seen in Figure 3b and Figure S5b that a total pressure of 24 bar (18 bar  $\text{CH}_4$ , 4 bar  $\text{CO}$ , and 2 bar  $\text{O}_2$ ) was desired, whereas higher or lower total pressure would lead to reduced  $\text{CH}_3\text{COOH}$  yield. As has been reported before, the influence of the ratios and pressures of reactants on the reaction can be complex,<sup>[4a, 4b]</sup> and fully understanding the mechanism and optimizing the reaction would be a significant undertaking that is beyond the scope of this present work. Nevertheless, it is important to note that our results indeed lay the groundwork for future research to further understand and optimize the process.

Guided by this set of parameters achieved through model reactions, we next carried out a 2-step process as shown in **Figure 1, right** by combining the  $\text{CO}_2$  reduction and  $\text{CH}_4$  oxidative carbonylation as described above. Briefly, the process started with loading the reactor with 18 bar  $\text{CH}_4$  and 8 bar  $\text{CO}_2$ , where 6 mg Rh-ZSM-5 (0.5 wt% Rh loading) was dispersed in 4 mL DI  $\text{H}_2\text{O}$ . In the inner reaction chamber, 7 mL electrolyte containing 0.1 M  $\text{KHCO}_3$  was used; the cathode was CoPc, and the anode was  $\text{IrO}_2$ , as detailed in the SI. A constant current density of 11.1  $\text{mA}/\text{cm}^2$  was first applied for 22 h at room temperature, during which 4 bar  $\text{CO}$  and 2 bar  $\text{O}_2$  were produced. Afterwards, the electrolysis was stopped, and the reactor was brought to 150 °C and maintained at this temperature for 3 h. At the end, *ca.* 3.2  $\text{mmol}/\text{g}_{\text{cat}}$   $\text{CH}_3\text{COOH}$  with a selectivity of 83% was detected (Figure S6). The yield was approximately 46% of what was obtained if the reaction was carried out in a single step with 18 bar  $\text{CH}_4$ , 4 bar  $\text{CO}$ , and 2 bar  $\text{O}_2$ . Possible reasons for the reduced yield include the presence of  $\text{CO}_2$  in the reaction medium, the existence of  $\text{H}_2$  byproducts as a result of the hydrogen evolution reaction (*ca.* 0.6 bar, Figure S7). To assess the influence of the oxidative carbonylation by the presence of  $\text{CO}_2$  and  $\text{H}_2$ , the following control experiments were performed. As shown in Figure S8, with the addition of 4 bar  $\text{CO}_2$  to the standard gases used for thermocatalysis, the yield of  $\text{CH}_3\text{COOH}$  was slightly lower (by 6%). The addition of 0.5 bar  $\text{H}_2$ , on the other hand, led to a significant decrease of the yield (by 32%). With both 4 bar  $\text{CO}_2$  and 0.5 bar  $\text{H}_2$  added, a 52% yield reduction was observed. It is important to note that no significant change to the product selectivity was measured in all these experiments. Taken together, we concluded that the key culprit for the decreased yield of the integrated experiment was due to the presence of  $\text{H}_2$ , although there appeared to be a synergistic effect between  $\text{CO}_2$  and  $\text{H}_2$ . Future research should focus on enhancing the selectivity of  $\text{O}_2$ -tolerent  $\text{CO}_2$  reaction catalysts to further suppress  $\text{H}_2$  production.

Our next task was to prove that the product was indeed the coupling of  $\text{CH}_4$  and  $\text{CO}_2$ . For this purpose, we employed  $^{13}\text{CO}_2$  as an isotope label for product analysis using  $^{13}\text{C}$  nuclear magnetic resonance ( $^{13}\text{C}$  NMR) (Figure 4). Both isotope-labelled and control experiments were carried out under the same conditions as detailed in the previous paragraph. Since the chemical shift of  $(^{13}\text{CH}_3)_2\text{SO}$  (39.4 ppm) in  $^{13}\text{C}$  NMR spectrum can be readily distinguished from those of the liquid products,  $(\text{CH}_3)_2\text{SO}$  (30  $\mu\text{L}$ ) was added to the collected reaction solution as an internal standard to compare the amounts of isotope-labelled products. Low intensity  $^{13}\text{CH}_3\text{COOH}$  ( $\delta = 21.3$  ppm) and  $\text{CH}_3^{13}\text{COOH}$

( $\delta = 180.0$  ppm) were detected in the control reactions with unlabeled  $\text{CO}_2$  due to the natural abundance (1.1%) of  $^{13}\text{C}$  (Figure 4, top). In stark contrast, the peak corresponding to  $\text{CH}_3^{13}\text{COOH}$  was much more pronounced in the products of the  $^{13}\text{CO}_2$ -labeled reaction, strongly supporting that the carbonyl group in  $\text{CH}_3\text{COOH}$  is derived from  $\text{CO}_2$  (Figure 4, bottom). By comparison, the peak of  $^{13}\text{CH}_3\text{COOH}$  was negligible in the  $^{13}\text{CO}_2$ -labeled reaction products, suggesting that the methyl group is from unlabeled  $\text{CH}_4$  (Figure 4, bottom). Furthermore, due to the high selectivity towards the formation of  $\text{CH}_3\text{COOH}$  under the integrated reaction conditions, only small amount of  $\text{HCOOH}$  and  $\text{CH}_3\text{OH}$  were detected (Figure 4 and Figure S9). Based on these isotope-labelled results, we confirmed that the formation of  $\text{CH}_3\text{COOH}$  was from the product of  $\text{CH}_4$  carboxylation with activated  $\text{CO}_2$ .

In conclusion, we have demonstrated the direct synthesis of  $\text{CH}_3\text{COOH}$  with high selectivity from two greenhouse gases  $\text{CH}_4$  and  $\text{CO}_2$  via integrated electrocatalytic  $\text{CO}_2\text{RR}$  and OER by an oxidative  $\text{CH}_4$  carbonylation mechanism. While most  $\text{CO}_2\text{RR}$  studies have overlooked the counter reactions, we have presented the direct utilization of the overall products to synthesize a meaningful compound under industrially relevant conditions. The reaction is atomically efficient, with  $\text{H}_2\text{O}$  being the only other chemical that is directly involved in the reaction which is recovered at the end of the catalytic cycle. Isotope studies confirm the coupling reaction between  $\text{CH}_4$  and activated  $\text{CO}_2$ . This study shows that the integrated route is an alternative to the existing processes that require the reforming of  $\text{CH}_4$  and the utilization of highly toxic gases such as  $\text{CO}$ . The result proves the concept of electrocatalytically activating a thermodynamically stable molecule ( $\text{CO}_2$ ) and directly using the products without the need of separation or transportation of the intermediates. This proof-of-concept work makes it possible to take advantage of parallel efforts in  $\text{CO}_2$  reduction by, for examples,  $\text{O}_2$ -tolerant  $\text{CO}_2\text{RR}$  catalytic systems with high selectivity, and electrolyte-free electrolysis methods.<sup>[15]</sup> Given the broad utilities of oxidative carbonylation in synthetic chemistry, our reported approach is expected to readily find ready applications.

## Supplementary Material

Refer to Web version on PubMed Central for supplementary material.

## Acknowledgements

The project was mainly supported by the National Science Foundation (CHE 1955098). The NMR efforts in this work were supported by the NSF MRI award CHE2117246, and the NIH HEI-S10 award 1S10OD026910-01A1. We thank Dr. Haochuan Zhang for his help with the XPS measurements at the Center for Nanoscale Systems at Harvard University, which is supported by the NSF award No. 1541959. We also thank Prof. Matthias Waegelé for his help with CO-DRIFTS.

## References

- [1]. Tang Y, Li Y, Tao F, Chem. Soc. Rev 2022, 51, 376–423. [PubMed: 34904592]
- [2]. Yoneda N, Kusano S, Yasui M, Pujado P, Wilcher S, Appl. Catal. A: Gen 2001, 221, 253–265.
- [3]. Sunley GJ, Watson DJ, Catal. Today 2000, 58, 293–307.
- [4]. a) Shan J, Li M, Allard LF, Lee S, Flytzani-Stephanopoulos M, Nature 2017, 551, 605–608; [PubMed: 29189776] b) Tang Y, Li Y, Fung V, Jiang D.-e., Huang W, Zhang S, Iwasawa Y, Sakata T, Nguyen L, Zhang X, Frenkel AI, Tao F, Nat. Commun 2018, 9, 1231; [PubMed: 29581429] c) Wu B, Lin TJ, Lu ZX, Yu X, Huang M, Yang RO, Wang CQ, Tian C, Li J, Sun YH,

Zhong LS, Chem 2022, 8, 1658–1672;d) Qi GD, Davies TE, Nasrallah A, Sainna MA, Howe AGR, Lewis RJ, Quesne M, Catlow CRA, Willock DJ, He Q, Bethell D, Howard MJ, Murrer BA, Harrison B, Kiely CJ, Zhao XL, Deng F, Xu J, Hutchings GJ, Nat. Catal 2022, 5, 45–54;e) Lin M, Sen A, Nature 1994, 368, 613–615.

- [5]. a) Zhao YT, Cui CN, Han JY, Wang H, Zhu XL, Ge QF, J. Am. Chem. Soc 2016, 138, 10191–10198; [PubMed: 27452233] b) Montejo-Valencia BD, Pagan-Torres YJ, Martinez-Inesta MM, Curet-Arana MC, ACS Catal. 2017, 7, 6719–6728;c) Zhao YT, Wang H, Han JY, Zhu XL, Mei DH, Ge QF, ACS Catal. 2019, 9, 3187–3197;d) Liu GX, Ariyaratna IR, Ciborowski SM, Zhu ZG, Miliordos E, Bowen KH, J. Am. Chem. Soc 2020, 142, 21556–21561. [PubMed: 33307694]
- [6]. a) Tu CY, Nie XW, Chen JGG, ACS Catal. 2021, 11, 3384–3401;b) Rabie AM, Betiha MA, Park SE, Appl. Catal. B 2017, 215, 50–59.
- [7]. a) Wang L, Yi Y, Wu C, Guo H, Tu X, Angew. Chem. Int. Ed 2017, 56, 13679–13683;b) Liu S, Winter LR, Chen JGG, ACS Catal. 2020, 10, 2855–2871;c) Shavi R, Ko J, Cho A, Han JW, Seo JG, Appl. Catal. B 2018, 229, 237–248.
- [8]. a) Meng XG, Cui XJ, Rajan NP, Yu L, Deng DH, Bao XH, Chem 2019, 5, 2296–2325;b) Jin Z, Wang L, Zuidema E, Mondal K, Zhang M, Zhang J, Wang CT, Meng XJ, Yang HQ, Mesters C, Xiao FS, Science 2020, 367, 193–197; [PubMed: 31919221] c) Nitopi S, Bertheussen E, Scott SB, Liu XY, Engstfeld AK, Horch S, Seger B, Stephens IEL, Chan K, Hahn C, Norskov JK, Jaramillo TF, Chorkendorff I, Chem. Rev 2019, 119, 7610–7672; [PubMed: 31117420] d) Liang SY, Huang L, Gao YS, Wang Q, Liu B, Adv. Sci 2021, 8, 2102886;e) Wu YS, Jiang Z, Lu X, Liang YY, Wang HL, Nature 2019, 575, 639–642. [PubMed: 31776492]
- [9]. a) Qiao JL, Liu YY, Hong F, Zhang JJ, Chem. Soc. Rev 2014, 43, 631–675; [PubMed: 24186433] b) Wang GX, Chen JX, Ding YC, Cai PW, Yi LC, Li Y, Tu CY, Hou Y, Wen ZH, Dai LM, Chem. Soc. Rev 2021, 50, 4993–5061; [PubMed: 33625419] c) Nielsen DU, Hu X-M, Daasbjerg K, Skrydstrup T, Nat. Catal 2018, 1, 244–254.
- [10]. a) Pan Y, Lin R, Chen Y, Liu S, Zhu W, Cao X, Chen W, Wu K, Cheong W-C, Wang Y, Zheng L, Luo J, Lin Y, Liu Y, Liu C, Li J, Lu Q, Chen X, Wang D, Peng Q, Chen C, Li Y, J. Am. Chem. Soc 2018, 140, 4218–4221; [PubMed: 29517907] b) Wang M, Torbensen K, Salvatore D, Ren S, Joulié D, Dumoulin F, Mendoza D, Lassalle-Kaiser B, I ci U, Berlinguette CP, Robert M, Nat. Commun 2019, 10, 3602. [PubMed: 31399585]
- [11]. Jensen MT, Rønne MH, Ravn AK, Juhl RW, Nielsen DU, Hu X-M, Pedersen SU, Daasbjerg K, Skrydstrup T, Nat. Commun 2017, 8, 489. [PubMed: 28887452]
- [12]. a) Zhang X, Wu Z, Zhang X, Li L, Li Y, Xu H, Li X, Yu X, Zhang Z, Liang Y, Wang H, Nat. Commun 2017, 8, 14675; [PubMed: 28272403] b) Matheu R, Gutierrez-Puebla E, Monge MÁ, Diercks CS, Kang J, Prévot MS, Pei X, Hanikel N, Zhang B, Yang P, Yaghi OM, J. Am. Chem. Soc 2019, 141, 17081–17085. [PubMed: 31613614]
- [13]. Lee Y, Suntivich J, May KJ, Perry EE, Shao-Horn Y, J. Phys. Chem. Lett 2012, 3, 399–404. [PubMed: 26285858]
- [14]. <j/>a). Lu X, Jiang Z, Yuan X, Wu Y, Malpass-Evans R, Zhong Y, Liang Y, McKeown NB, Wang H, Sci. Bull. 2019, 64, 1890–1895.b) Xu Y, Edwards JP, Zhong J, O'Brien CP, Gabardo CM, McCallum C, Li J, Dinh C-T, Sargent EH, Sinton D. Energy Environ. Sci 2020, 13, 554–561.c) Li P, Lu X, Wu Z, Wu Y, Malpass-Evans R, McKeown NB, Sun X, Wang H. Angew. Chem. Int. Ed 2020, 59, 10918–10923.
- [15]. Selt M, Franke R, Waldvogel SR, Org. Process Res. Dev 2020, 24, 2347–2355.



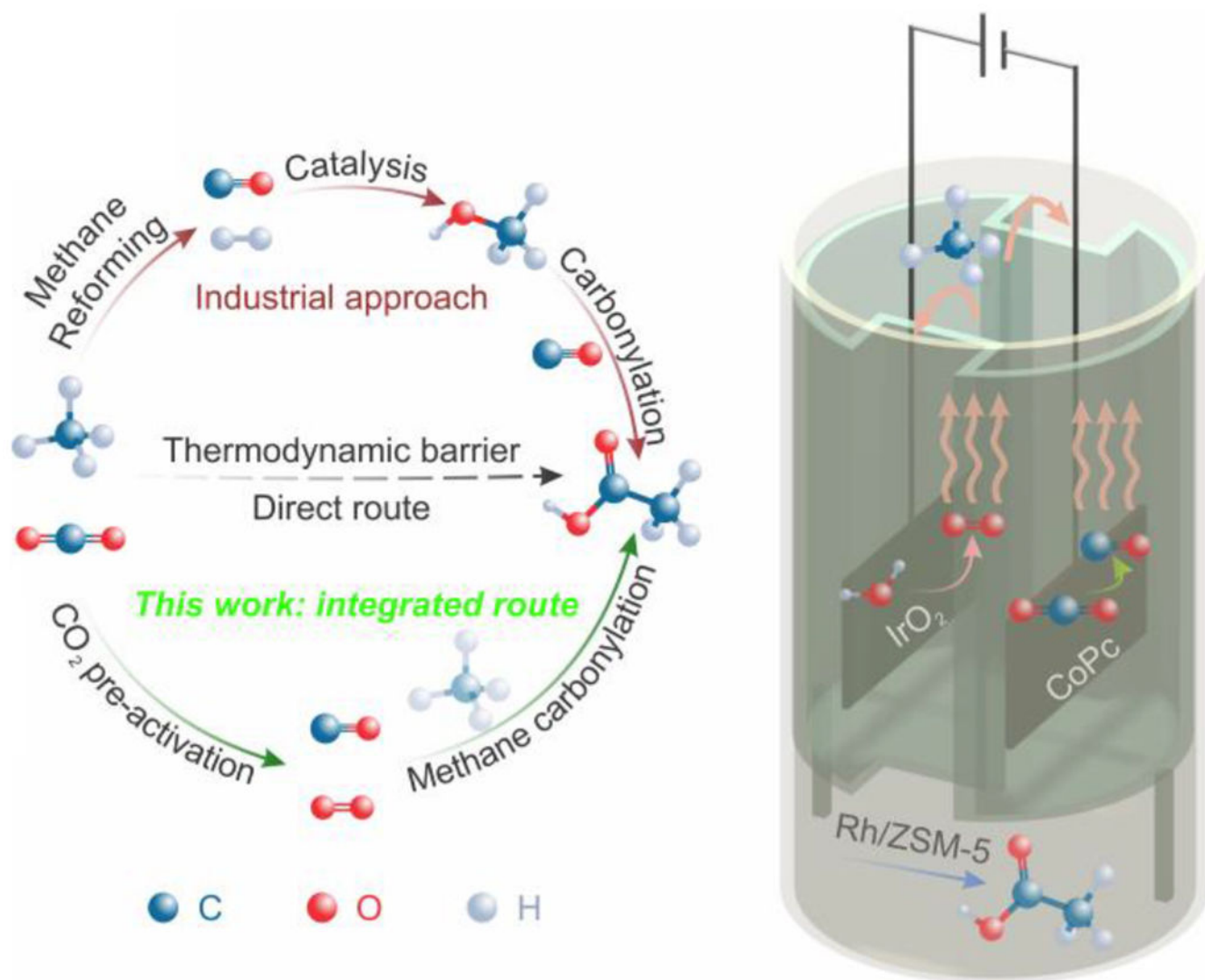


**Figure 1.** Overview of our design. **Left:** Different routes to synthesize CH<sub>3</sub>COOH. **Right:** Schematic illustration of an integrated route via electrocatalytic conversion of CO<sub>2</sub> to CO and subsequent thermocatalytic methane carbonylation to synthesize CH<sub>3</sub>COOH.

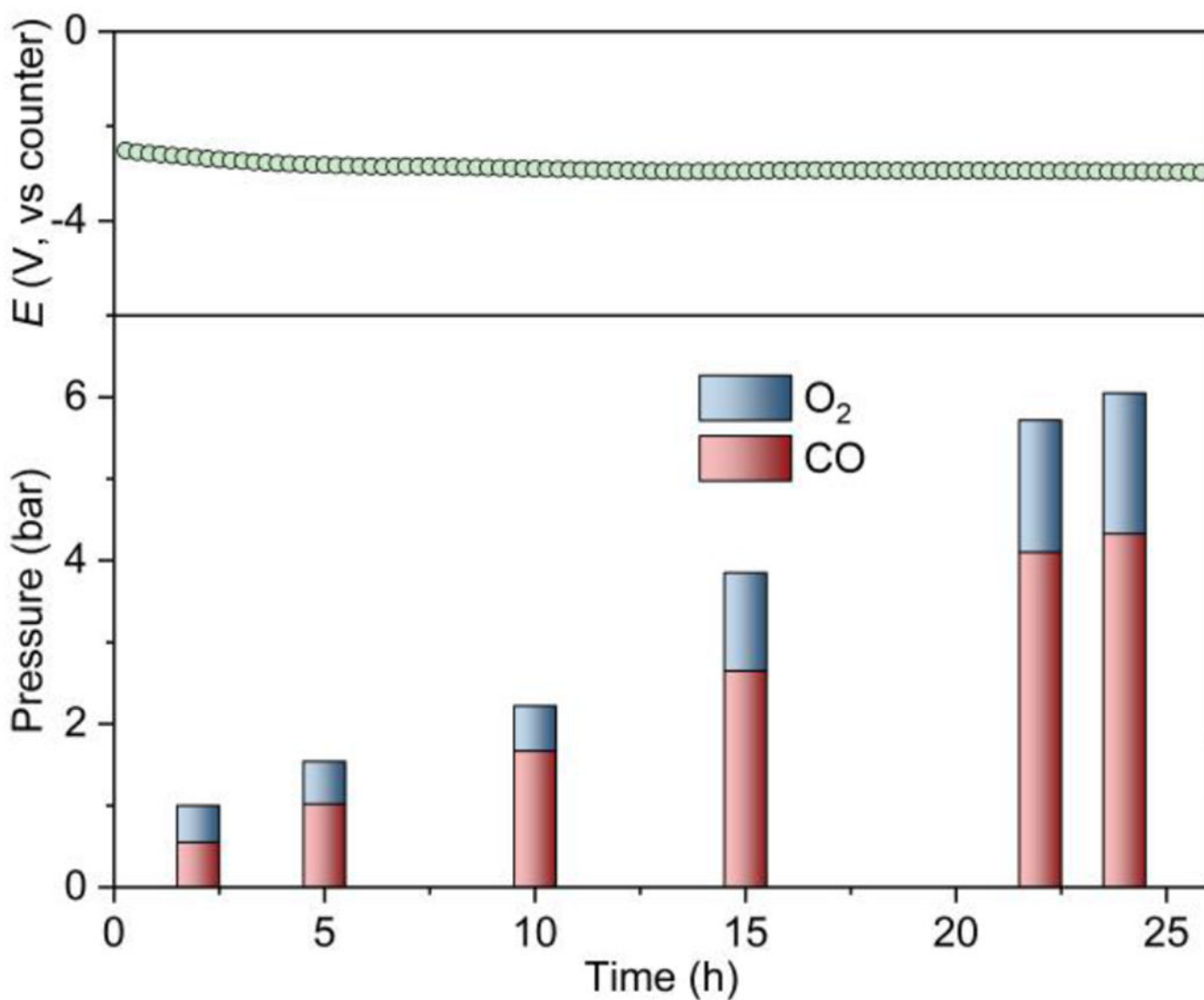


**Figure 2.** Electrochemical reduction of CO<sub>2</sub> and the production of CO and O<sub>2</sub>. **Top:** Voltage evolution during the electrocatalytic CO<sub>2</sub>RR with a constant current of 11.1 mA/cm<sup>2</sup>. The data are *iR* corrected. **Bottom:** CO and O<sub>2</sub> pressures at different electrocatalytic CO<sub>2</sub>RR times with an initial CO<sub>2</sub> pressure of 8 bar and CH<sub>4</sub> pressure of 18 bar.

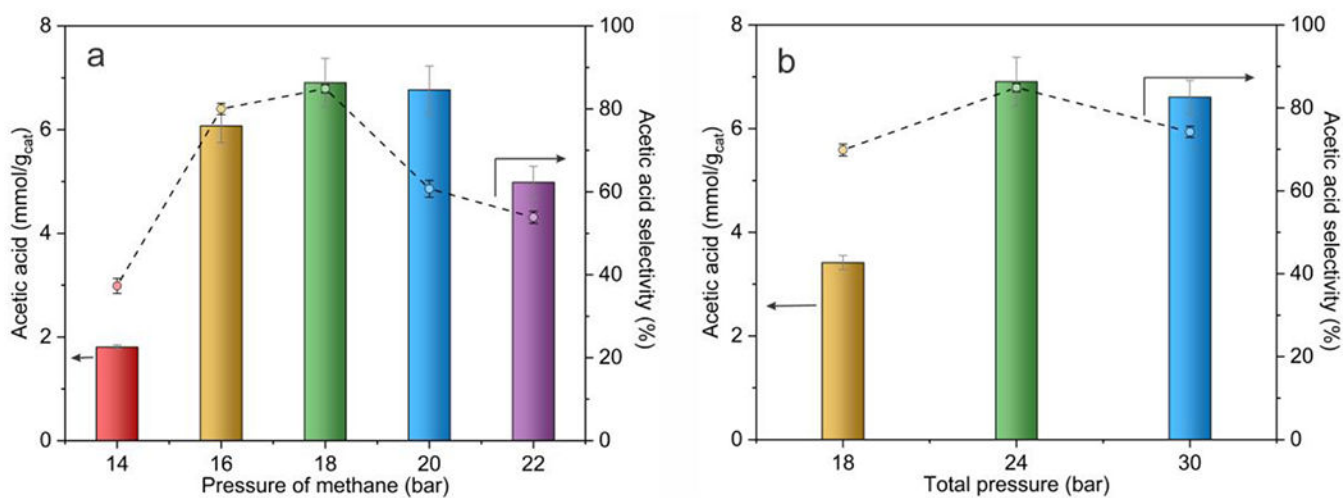


**Figure 3.**

Influence of pressures of CH<sub>4</sub>, CO, and O<sub>2</sub> on the yield of CH<sub>3</sub>COOH. Reaction conditions: 16 mg of catalyst, 3-5 bar of CO, 1.5-2.5 bar of O<sub>2</sub>, 11 mL of water, 3 h of reaction at 150 °C. (a) Dependence on the pressure of CH<sub>4</sub> when  $P_{CO}$  is fixed at 4 bar and  $P_{O_2}$  is fixed at 2 bar. (b) Dependence on the total pressure with  $P_{CH_4}:P_{CO}:P_{O_2}$  is fixed at 9:2:1. The CH<sub>3</sub>COOH selectivity represents that of all liquid products.

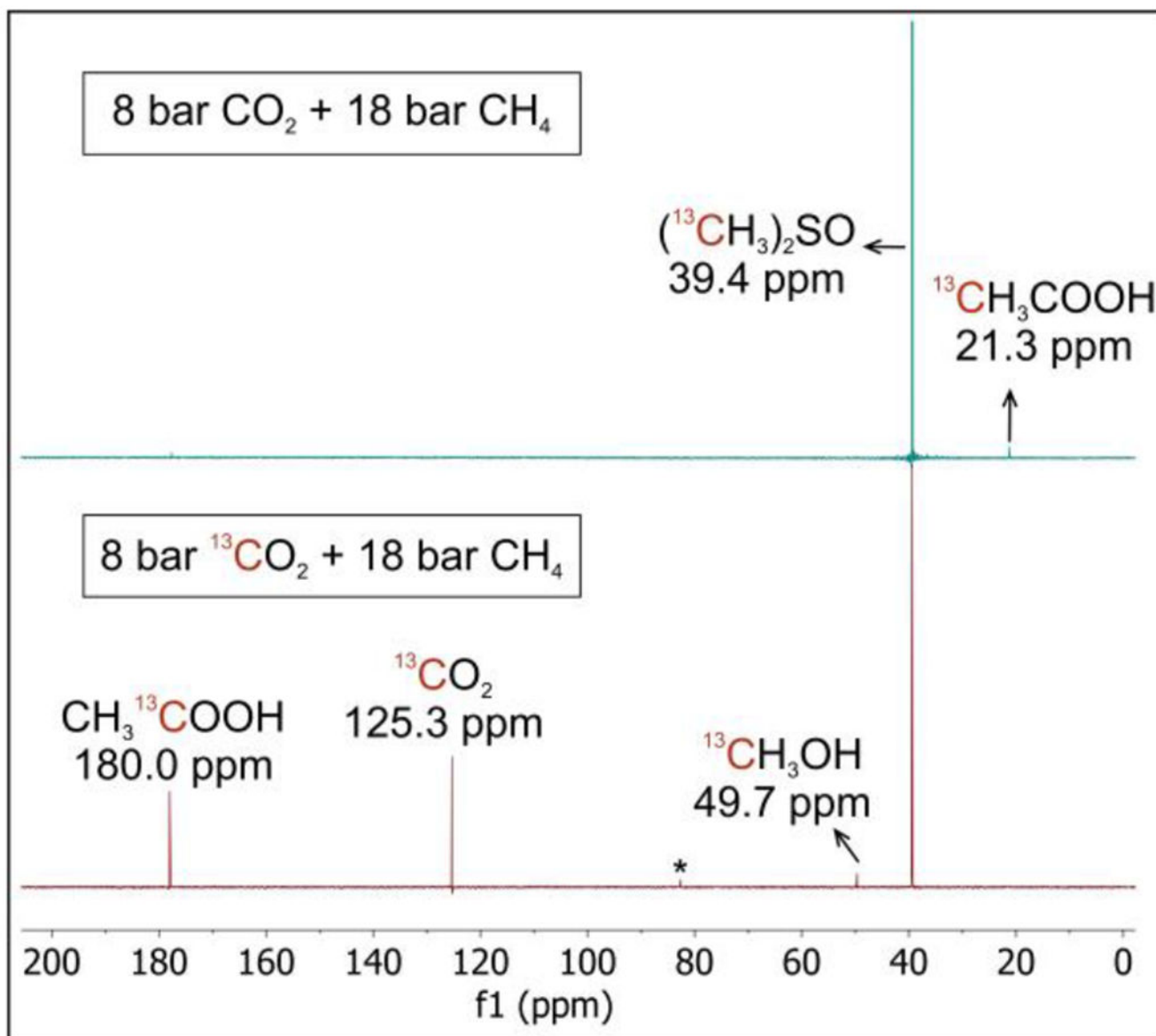


**Figure 4.**  
<sup>13</sup>C NMR spectra of the liquid products by reactions using CO<sub>2</sub> (**top**) and <sup>13</sup>CO<sub>2</sub> (**bottom**).  
\* indicates CH<sub>2</sub>(OH)<sub>2</sub>.